

# We are IntechOpen, the world's leading publisher of Open Access books Built by scientists, for scientists

6,900

Open access books available

185,000

International authors and editors

200M

Downloads

Our authors are among the

154

Countries delivered to

TOP 1%

most cited scientists

12.2%

Contributors from top 500 universities



WEB OF SCIENCE™

Selection of our books indexed in the Book Citation Index  
in Web of Science™ Core Collection (BKCI)

Interested in publishing with us?  
Contact [book.department@intechopen.com](mailto:book.department@intechopen.com)

Numbers displayed above are based on latest data collected.  
For more information visit [www.intechopen.com](http://www.intechopen.com)



## Chapter

# Open-Pore Foams Modified by Incorporation of New Phases: Multiphase Foams for Thermal, Catalytic and Medical Emerging Applications

*Lucila Paola Maiorano Lauría and José Miguel Molina Jordá*

## Abstract

Recently, open-pore foam materials have acquired great interest in several technological sectors due to their excellent properties of low density, great specific surface area, adjustable thermal conductivity, and high-energy absorption. The replication method has proved to be one of the most widely used techniques for their manufacture, allowing a perfect control of the pores' characteristics from which the main properties of the foams derive. However, these properties have limited the use of these materials in ultimate applications of the most demanding emerging technologies. This chapter reviews recent developments of open-pore foams that have been modified by the incorporation of new phases in order to enhance their properties. The inclusion of new phases taking part of the microstructure or modifying the pore surfaces allows these materials to be considered promising for the most modern applications including, among others, thermal dissipation, catalytic supports, and medical implantology.

**Keywords:** open-pore foam, multiphase foam, inclusions, thermal management, catalysis, medical implantology

## 1. Introduction

Foam materials were originally conceived by clear inspiration in some natural porous materials, such as wood, bamboo canes, or bones, as they present a very attractive combination of properties such as excellent mechanical strength blended with low density [1]. Motivated by the versatility of those natural porous materials, human ingenuity succeeded in the design of new foam materials, their most suitable manufacturing processes, and their use in technologically demanding applications. In recent years, foam materials have reached a high level of maturity in their manufacture, development, applications, and integration into complex systems to fulfill specific applications.

Foam materials can be classified depending on their nature, pore interconnectivity, morphology of their cellular structure, or other variables that allow their differences to be outlined. A widespread classification divides foams into open-pore

and closed-pore, depending on whether their porous cellular structures are interconnected or not, respectively. When more than half of the cells are open, the materials are considered open-pore foams. Closed-pore foams were proven useful in thermal insulation and structural applications (load-bearing components, energy absorbers, etc.) as well as in biomedical implants. Open-pore foams have cells that are not completely closed so a fluid can pass through the material. While open-pore foams are structurally less interesting, their open-pore space expands their utility to functional applications such as particle filters, bacteriological filters, active heat dissipation units, etc.

The fields of application of open-pore foam materials depend on their porous architectures and the nature of their solid phases. Open-pore ceramic foams have traditionally been used as thermal insulators, bio-scaffolds in tissue engineering, catalytic supports, and materials for sound and impact absorption, among others [2]. Recently, their use has been extended to catalytic applications given their suitability to be catalyst supports in gaseous or liquid phase reactions, since the presence of interconnected pores allows the passage of fluids and, therefore, can be used in continuous reactors. Polymer foams show excellent properties which make them suitable for many applications such as construction, cushioning and insulation, or sound dampening [3]. Open-pore metal foams also share some of these applications, but they deserve a special attention. Their outstanding mechanical and thermoelectrical conductive properties allow these materials being considered excellent candidates for a wide variety of applications depending on their porous structure, as it can be seen in **Figure 1**. Their high surface area per unit volume, low density, and great heat transfer capacity make them suitable for thermal management (heat exchangers and heat sinks), electrode materials, catalyst carriers, and biomedical engineering as biocompatible and biodegradable scaffolds [4]. When used in medical implantology, the interconnected structure provides a transition space between the bone and the biomaterial structural support, which allow the in-growth of bone tissue and vascularization [5]. Other properties such as high strength and toughness, great sound-absorbing capacity, and high impact energy

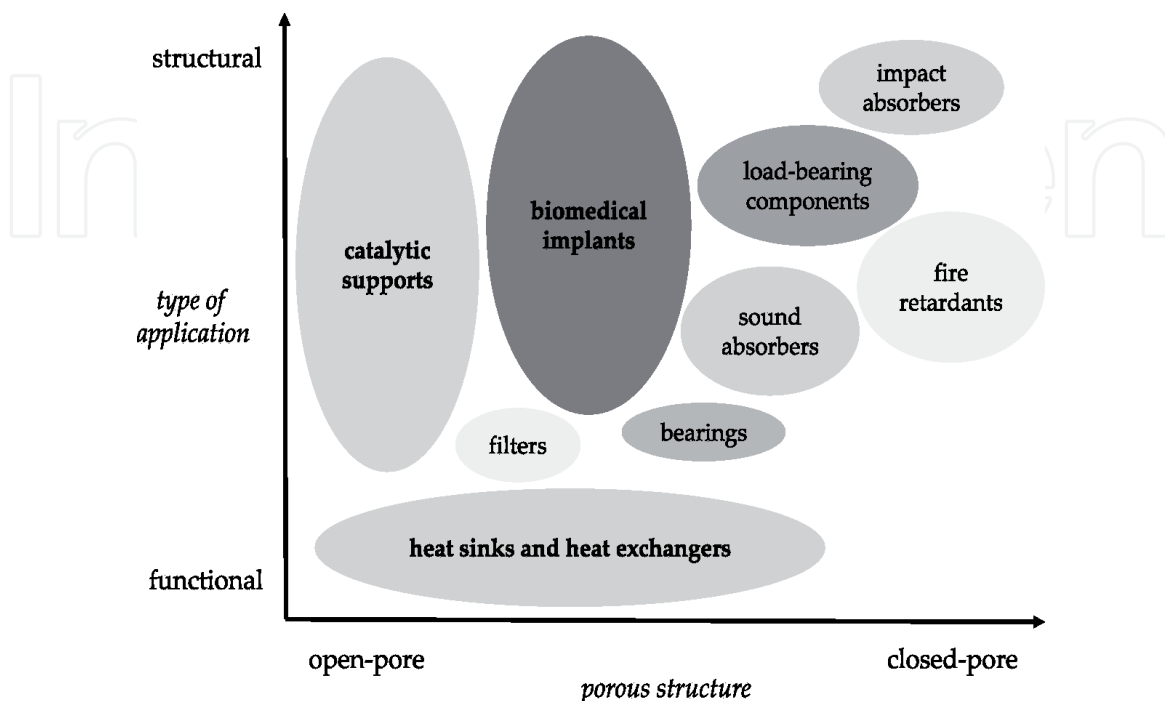


**Figure 1.** Applications of metal foams according to porous structure. Partially reproduced from [1].

absorption make them interesting materials for structural applications in the aerospace, automotive, or marine industry.

Despite all their great attributes, traditional foams are often inappropriate to meet the requirements of the most advanced technological challenges; hence their designs have recently been reformulated by the incorporation of new functional phases. In this work, the authors focus the attention on this last type of open-pore foams, in which different components/phases have been incorporated to generate multiphase materials with a great potential of use in applications of different sectors such as electronics, medicine, or catalysis.

## **2. Current needs to incorporate new phases into open-pore foams**

The development of emerging technologies such as new electronic devices in electronics, aeronautics, and aerospace; advances in the chemical industry; and the still incipient stage of biomedical engineering is concomitant with the accelerated progress of research into new materials. Some of the most demanding applications require further developments of open-pore foam materials and are discussed here below.

Thermal management has become a critical issue that often slows down or even hinders the progress of evolving power electronic technologies as a result of increasing power densities and decreasing transistor dimensions [4–8]. A successful strategy for efficient heat removal in electronic systems, called active thermal management, consists in forcing the direct transfer of heat from hot spots to some carrier fluids through a conduction-convection mechanism by means of using high thermally conductive open-pore foams. Research into new materials for these applications was focused mainly on metal and carbon/graphite foams as they exhibit interesting physical properties, such as low density and high specific area per unit volume, as well as decent thermal conductivity [9–12]. Many authors have focused on the investigation of forced convection parameters, such as heat transfer coefficient and pressure drop for different metal foams. Although these materials exhibit interesting characteristics, their properties of relatively high heat transfer coefficient and low pressure drop are still insufficient for its use in final applications of the most demanding emerging electronic technologies. Recent developments have modified open-pore foams by the incorporation of new phases either into the solid or into the cavities of the porous structure. These materials show considerable improvements in their thermal properties [8, 13, 14].

Open-pore foams used in catalytic applications must meet two requirements: a high specific surface allowing high dispersion of the catalytically active phase and not too small pore sizes to prevent a high pressure drop of the fluid passing through it. Although the open-pore foams used so far in catalysis have roughly met these characteristics, the new demands for better catalytic performance require materials with new structural pore designs and improved properties. To this end, porous materials must provide (i) the highest possible thermal conductivity to improve heat transport from or to the outside of the catalytic reactor (easily achievable when the nature of the solid is metallic) and (ii) the possibility to break the laminar flow in order to enhance the interaction between the fluid and the catalyst. The first requirement can be achieved by incorporating thermal inclusions into the solid phase of the foam and/or by a crystalline modification of the solid phase assisted by the catalytic action of the new present phases. The second requirement can be achieved by incorporating new phases into the porous cavities.

In addition to the mentioned applications, open-pore metal foams are recently being the subjects of intense study in medical implantology. These

materials are not only intended to fulfill a structural purpose in a body system but also to cover functional applications. It was recently proposed to incorporate guest phases in the porous cavities of open-pore foams charged with pharmacological substances, with the aim to set a drug delivery system to avoid postsurgical infections [15, 16].

By way of the commented examples, the authors intend to highlight that the inclusion of new phases into open-pore foams opens up a range of new properties in foam materials and seems to be a suitable way to overcome the requirements of modern applications such as some of those commented for thermal management, catalytic chemistry, and medical implantology. In addition, some research works focus on the incorporation of new phases into foams to enhance mechanical properties as in all the mentioned applications, better mechanical performances are also soaked.

### **3. Manufacture**

#### **3.1 Manufacturing techniques of open-pore foams**

Manufacturing techniques of open-pore foams can be classified into four groups attending to the state of the precursor material: liquid, solid, vapor, and ions [1].

**Liquid state processing:** the precursor material is in liquid state. The most important processing techniques are:

- a. Investment casting with polymer foams
- b. Casting around space holder materials/infiltration of martyr preforms

**Solid state processing:** the precursor material is in solid state. The following techniques are the most important ones:

- a. Partial sintering of powders and fibers
- b. Foaming of slurries
- c. Pressurization and sintering of powders in martyr preform
- d. Sintering of hollow spheres
- e. Sintering of powders and binders
- f. Reaction sintering of multicomponent systems

**Vapor state processing:**

- g. Vapor deposition onto polymeric foams

**Ionic solution state processing:**

- h. Electrodeposition onto polymeric foams

Despite the wide range of fabrication methods that these four groups generate, there are actually only two different strategies for generating porosity [17]:

- Self-formation: porosity is formed through a process of evolution according to the physical principles. Self-formation includes the d method.
- Predesign: the structure is created with the use of molds that determine the porous cavities. By means of this strategy, closed-pore (or not interconnected) and open-pore (or interconnected) foams can be manufactured, depending on whether the mold forms part of the final material or is removed, respectively. Predesign includes a, b, c, e, f, g, h, i, and j methods.

Among the manufacturing techniques, the infiltration of martyr preforms, also known as the replication (predesign) method, allows the best control over the material. This method was traditionally used to produce open-pore metal foams and recently adapted to produce carbon/graphite foams [18]. The replication method consists of the infiltration with molten metal or any other liquid precursors of a porous template preform that is later removed by dissolution or controlled reaction to leave a foam material with a porous structure that replicates the original preform. This method allows perfect control of size, shape, and size distribution of pores. Depending on the matrix material and the desired final porous architecture, different raw materials have been used as templates. Nevertheless, the most widespread martyr material is sodium chloride in particulate form, which can be conveniently packaged and infiltrated with liquid metals at temperatures below its melting point (801°C) and then removed by dissolution in aqueous solutions [13].

### 3.2 Manufacturing techniques of multiphase open-pore foams

The multiphase open-pore foam materials developed so far are still scarce and can be manufactured by various methods, which are reviewed in **Table 1** and later in the chapter.

#### 3.2.1 Composite foams/foams with guest phases with preload of new phases in the preform

Loading of new phases is achieved by one of the following two strategies: (i) loading particles (inclusions) are packed together with larger martyr particles forming a porous bimodal preform, or (ii) loading particles are covered by a martyr material and packed forming a porous monomodal preform. Preforms are infiltrated and the martyr material is leached away. As a result, composite foams or foams with guest phases are obtained. They show homogeneous dispersion of new phases in a continuous matrix. **Figure 2** represents the aforementioned material structures. In particular cases, loading powders are packed combined with larger martyr particles and sintered. The martyr particles are later removed to obtain an interconnected porous structure.

#### 3.2.2 Composite foams with preload of new phases in the liquid precursor

Loading of new phases is achieved by the dispersion of particles into the liquid precursor. The preform is leached away after its infiltration with the liquid precursor, and the final material shows a homogeneous dispersion of new phases in a continuous matrix. Material consolidation can also be obtained (instead of by infiltration) by electrochemical (co)-deposition of a metal and/or the new phases on a leachable preform or a preexistent porous material (the liquid precursor is an electrolyte that contains metal ions and dispersed particles of the new phases) (**Figure 3**).

Method	Inclusion into monolithic materials		Combination of monolithic materials			
	Material type	Composite foams/foams with guest phases	Composite foams	Finned foams	Monolithic finned foams	Composite finned foams
New phase loading		Preload in preform	Preload in liquid precursor	No preload	No preload	Preload in preform
Distribution of new phases		Homogeneous dispersion in matrix	Homogeneous dispersion in matrix and/or pore surface	Homogeneous dispersion in one component; layered distribution of components	Homogeneous dispersion in one component; layered distribution of components	Homogeneous dispersion in one component; layered distribution of components
Assembly		Combination of packed/self-standing preforms with liquid precursor or powders	Combination of packed/self-standing preforms with liquid precursor/electrodeposition	Physical or glue joining of preexistent monolithic materials	Casting of liquid precursor in a mold	Combination of packed/self-standing preforms with liquid precursor
Matrix continuity		Continuous	Continuous	Noncontinuous	Continuous	Continuous
References		[8, 13, 15, 16, 19]	[8, 14, 20–29]	[30–32]	[33]	[13]

**Table 1.**  
Methods currently developed to manufacture multiphase open-pore foams.

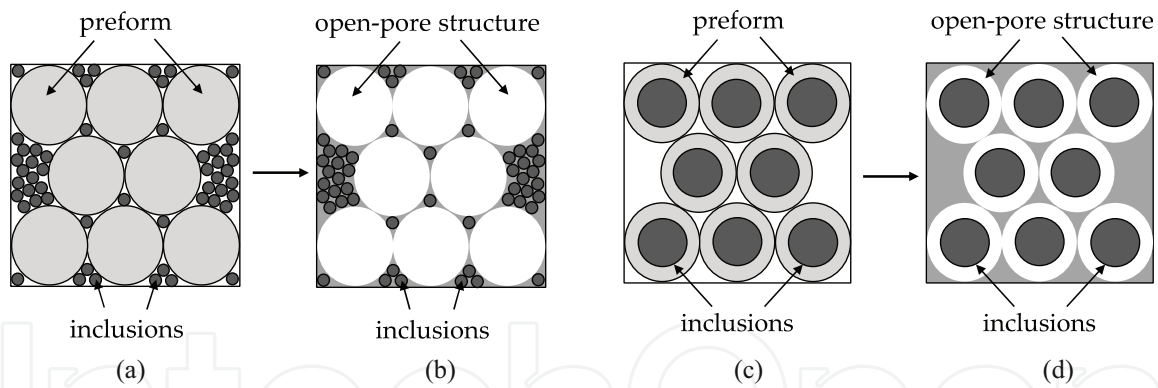


**Figure 2.** Schematic drawings showing preform compositions (a and c) and the structures of the final materials (b and d) for composite foams (a and b) and foams with guest phases (c and d) obtained by preload of new phases in the preform.

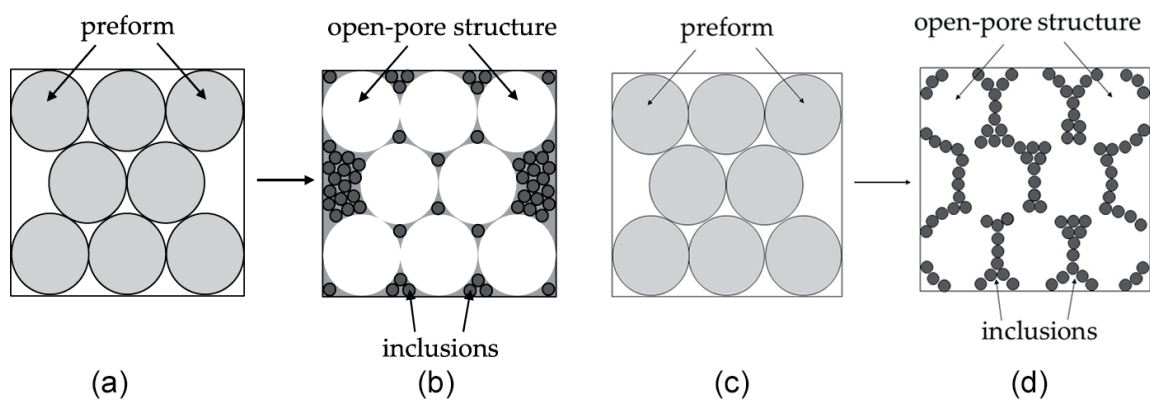


**Figure 3.** Schematic drawings showing preform compositions (a and c) and the structures of the final materials (b and d) for composite foams obtained by preload of new phases in the liquid precursor processed by infiltration (a and b) or by electrochemical (co)-deposition (c and d).

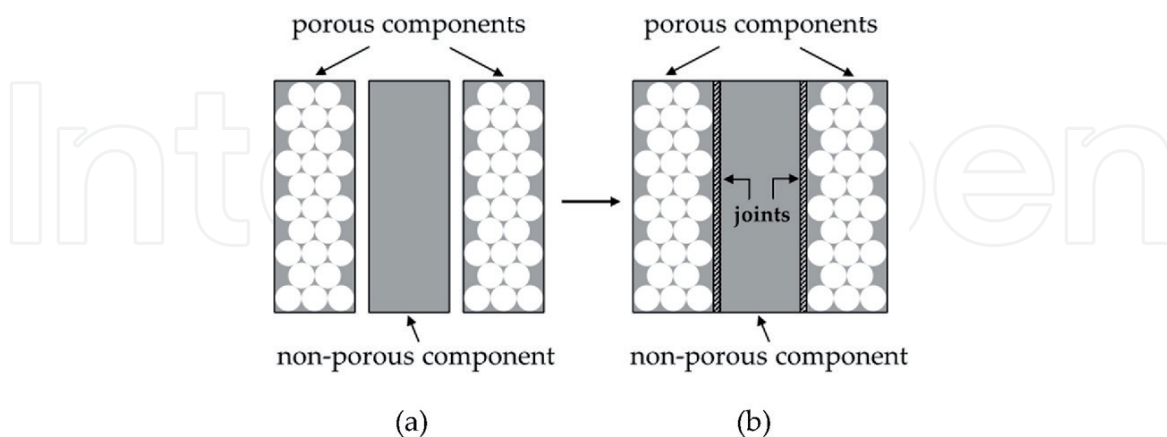


**Figure 4.** Schematic drawings showing component composition (a) and the structure of the final material after components joining (b) for finned foams.

### 3.2.3 Finned foams

Finned foams are normally manufactured by physical bonding or by gluing preexistent monolith layers (herein called components) of porous and nonporous materials. The nonporous materials are considered the new phases which are

integrated into a material with a layered structure and a noncontinuous matrix (joints are present in between components) (**Figure 4**).

### 3.2.4 Monolithic finned foams

Another way to fabricate finned foams is to perform a casting of a liquid precursor into a mold where preexistent self-standing porous leachable preforms are conveniently located. As a result, monolithic finned foam materials with continuous matrix can be obtained (**Figure 5**).

### 3.2.5 Composite finned foams

Loading of new phases is achieved by building an assembly consisting of packed or self-standing porous leachable preforms alternated with packed beds of the new phases in finely divided form (inclusions). After infiltration and removal of the leachable materials, a final material with a layered distribution of components and continuous matrix is obtained (**Figure 6**).

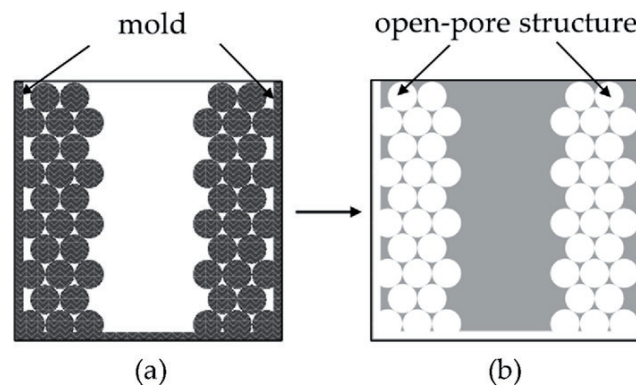


**Figure 5.** Schematic drawings showing a mold with preexistent self-standing porous leachable preforms (a) and the structure of the final material (b) for monolithic finned foams.

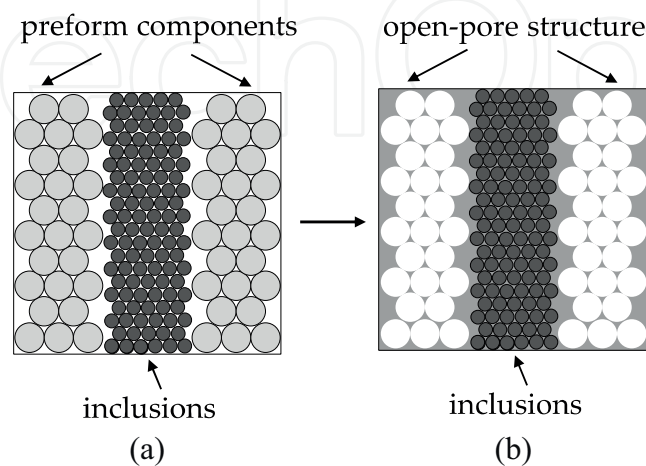


**Figure 6.** Schematic drawings showing an assembly consisting of packed or self-standing porous leachable preforms alternated with packed beds of finely divided inclusions (a) and the structure of the final material (b) for composite finned foams.

## 4. Multiphase open-pore foams: examples and properties

### 4.1 Composite foams/foams with guest phases with preload of new phases in the preform

#### 4.1.1 Magnesium/diamond composite foams

Open-pore magnesium foams, which have traditionally been discarded for active thermal management due to their low thermal conductivity values, can be appropriate for heat dissipation applications if they incorporate thermal inclusions such as diamond particles coated with a TiC layer of nanometric dimensions. These multiphase open-pore composite foams can be manufactured by the replication method following a strict processing control. First, a correct distribution of the preform components (NaCl and diamond particles) has to be achieved to ensure homogeneity and complete connectivity of the pores after dissolution. For this purpose, the selection of the composition of bimodal particle mixtures has been studied in detail following a predictive method described in [8, 34–37]. The results of these calculations are depicted in **Figure 7a** for the entire spectrum of NaCl particle fraction in the bimodal mixtures. The complete pore connectivity is achieved when the composition of NaCl in the bimodal (NaCl-diamond) mixture falls in the region of interest represented in **Figure 7a**. In this region the large NaCl particles are touching each other, and the smaller diamond particles are filling the voids left by the sodium chloride particles.

Another critical processing step is the proper control of TiC coating on diamond particles, which allows for high thermal conductance at the interface between the diamond particles and the matrix. The scanning electron microscopy (SEM) images in **Figure 8** illustrate some microstructural features of Mg/diamond composite foam. **Figure 8a** shows the diamond particles homogeneously distributed in the struts of the Mg matrix. **Figure 8b** depicts Si and Fe precipitates on diamond surfaces. During the metal solidification, traces of Si and Fe present in the nominal composition of magnesium segregate toward the interface, enhancing together with the TiC coating the magnesium-diamond interfacial thermal conductance.

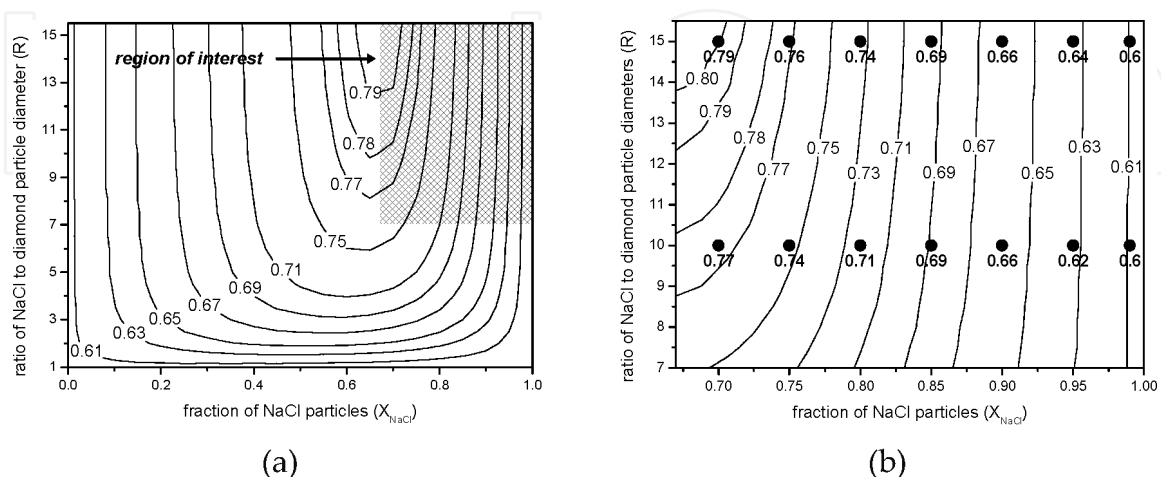


**Figure 7.** Contour diagram of the total volume fraction of inclusions (considering diamond and salt particles mixtures) over the whole range of NaCl particle fraction ( $X_{\text{NaCl}}$ ) as a function of  $R$  (ratio of the diameters of coarse NaCl particles to small diamond particles) (a); (b) is a magnification of the region of interest show in (a). Reproduced with permission from [8].

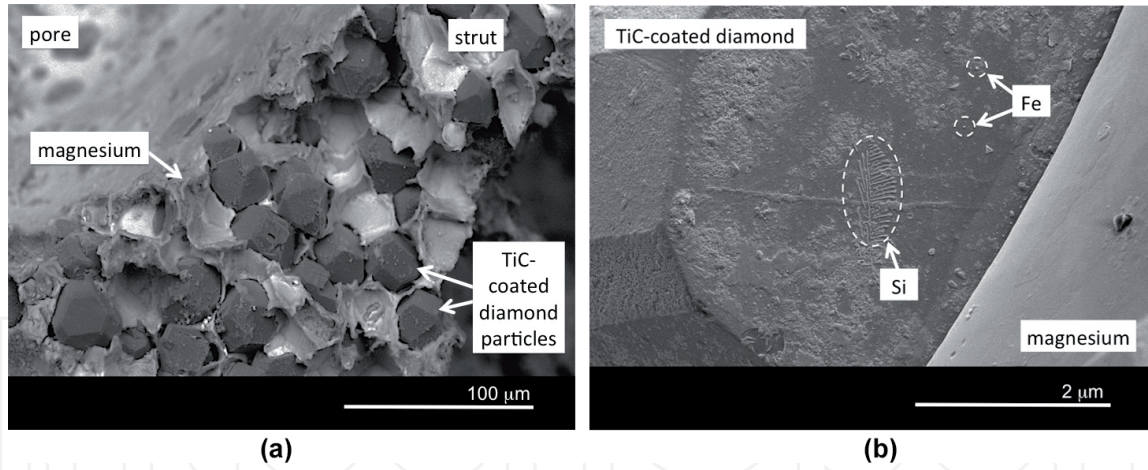


**Figure 8.** SEM micrographs of TiC-coated diamond particle distribution in the foam struts (a) and fine precipitates of silicon and iron on the TiC-coated diamond particles (b). Sample (a) was prepared by fracture, while sample (b) was prepared by fracture followed by magnesium electro-etching. Reproduced with permission from [8].

The thermal conductivity of these materials was both measured and estimated with analytical methods. The measurement of the thermal conductivity was carried out by the so-called comparative stationary method, which provides accurate and relatively fast measurements. It consists of comparing the thermal conductivity of an unknown material (the sample) with that of a reference, connecting the sections of both and establishing a thermal gradient.

The thermal conductivity was estimated with the differential effective medium (DEM) scheme, which has been extendedly applied with success to model and interpret thermal conduction in different composite materials consisting of randomly distributed monodispersed particles in a metal matrix [8, 34, 35, 37, 38]. The leading equation is expressed as the following integral:

$$\int_{K_m}^{K_C} \frac{dK}{K \sum_i X_i \frac{-(K - K_r^{eff})}{(K - K_r^{eff})^p - K}} = -\ln(1 - V) \quad (1)$$

where  $K$  is thermal conductivity and subscripts  $C$  and  $m$  refer to composite and matrix, respectively.  $X_i$  is the fraction of the  $i$  inclusion type in the total amount of inclusions of the composite (in composites containing only one type of inclusions  $i = 1$ ; hence,  $X_1 = 1$ ).  $V$  is the total volume fraction of inclusions, and  $p$  is the polarization factor of an inclusion (equal to one-third for spheres).  $K_r^{eff}$  is the effective thermal conductivity of an inclusion which, for spherical geometries, is related to its intrinsic thermal conductivity,  $K_r^{in}$ , the matrix/inclusion interface thermal conductance  $h$ , and the radius of the inclusion  $r$ , by

$$K_r^{eff} = \frac{K_r^{in}}{1 + \frac{K_r^{in}}{hr}} \quad (2)$$

In general, the integral on the left-hand side of Eq. (1) has no analytical solution and needs to be solved numerically with appropriate mathematical software.

Foam materials can be considered composites where pores are inclusions of zero nominal thermal conductivity ( $K_r^{in} = 0$  W/mK). Eq. (1) then becomes

$$K_C = K_{foam} = K_m (1 - V_p)^{\frac{1}{1-p}} \quad (3)$$

where  $V_p$  refers to the volume fraction of pores and  $p$  is now the polarization factor of the pores (equal to the polarization factor of the NaCl particles from which

the pore structure of the foam was derived, since the replication method maintains the morphological characteristics of the leachable particles in the pores of the final material). For spherical particles again  $p = 1/3$  [8]; in more complicated particle geometries, the value of  $p$  can be derived from the slope of a plot of  $\log(K_{foam})$  vs.  $\log(1 - V_p)$  for foam materials in which  $V_p$  is varied.  $K_m$  is the thermal conductivity of the matrix in the foam material, which can be in turn calculated with Eq. (1) by considering that the matrix is an effective composite material of pure magnesium with diamond particles as thermal inclusions.

The calculated thermal conductivities of Mg/diamond composite foams according to Eqs. (1)–(3) are plotted in **Figure 9a** against the experimental results [8]. In general, large fractions and large average sizes of diamond particles in the matrix generate higher thermal conductivities, and the presence of nano-coated TiC diamond is necessary to overcome the thermal conductivity of magnesium foam, reaching values up to 82 W/mK when the material contains 30% of nano-coated TiC diamond.

Since there is no standardized methodology for testing heat sinks in induced-convection active thermal management, the author of [8] proposed a new experimental setup inspired by that reported in [39] to measure power dissipation density of open-pore materials. Results obtained with this setup showed that composite foams achieved excellent performance in active thermal management with values up to 100% higher than their equivalent magnesium foams and 20% superior than conventional aluminum foams (**Figure 9b**).

#### 4.1.2 Aluminum/graphite flake composite foams

These multiphase foam materials were inspired by the recently developed family of highly anisotropic thermally conductive ternary composites formed by the combination of graphite flakes (Gf), ceramic particles, and a metal matrix [40, 41]. Aluminum/graphite flake (Al/Gf) composite foams combine the appeal of using Gf to improve thermal conductivity with the advantages of metal foams and configure a new family of foam materials with great potential for active thermal management applications. These materials are fabricated using the replication method, replacing the ceramic particles of the ternary composites with

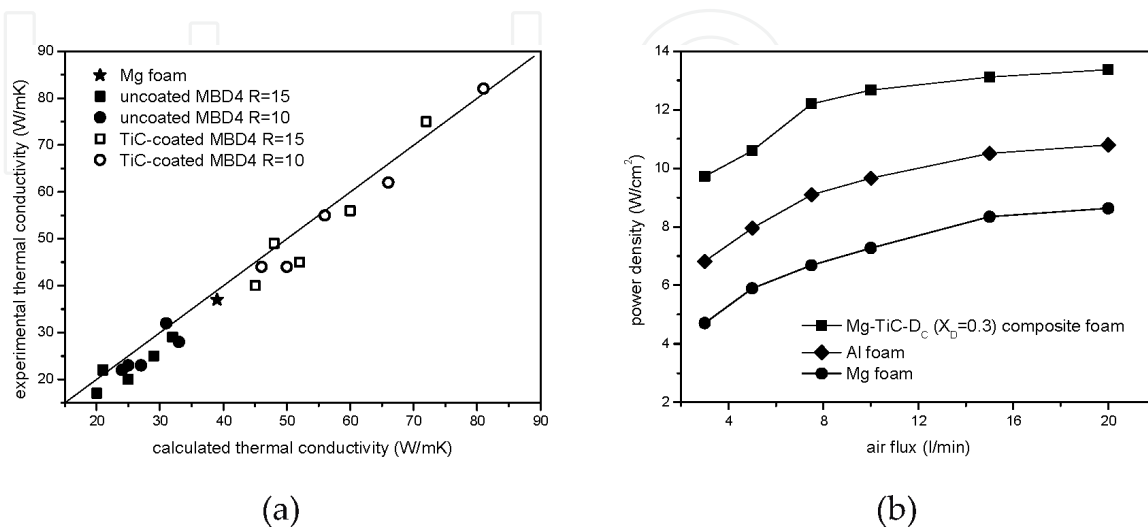


**Figure 9.** Experimental vs. calculated thermal conductivities for Mg/diamond composite foams developed in [8] (a) and a comparison of power density as a function of airflow between Mg-TiC/diamond composite foam and conventional metal foams (b). In (a), MBD4 refers to the quality of the diamond particles; in (b),  $X_D$  is the diamond particles fraction in the original bimodal particle mixture preform. Reproduced with permission from [8].

sodium chloride particles, which act as templates and can be removed by dissolution to obtain a material with an interconnected porous structure. The preforms were prepared by packing under external pressure a homogeneous distribution of oriented Gf and NaCl particles.

Two restrictions were found according to the preparation of these preforms. The first one was related with the dissolution of the template. To ensure complete and effective dissolution, the NaCl particles must achieve a coordination number for each particle of at least 3. This restriction defined a so-called percolation limit that is shown in **Figure 10a** as a dotted straight line. The second restriction has to do with the existence of a minimum volume fraction attained when particles are subjected to the sole action of gravity. This second restriction, the so-called compaction limit, is represented in **Figure 10a** by the line corresponding to a nominal zero pressure. As a consequence, preforms with compositions falling in regions below these two limits of **Figure 10a** cannot be manufactured.

For these microstructures where Gf are oriented and distributed homogeneously in a matrix, we can take the following expression for the longitudinal thermal conductivity of composite foams  $K_C^L$  [13, 41]:

$$K_C^L = K_{foam} + K_{foam} \frac{V' f}{\frac{\pi t}{4D}(1 - V' f) + \frac{K_{foam}}{K_f^L - K_{foam}}} \quad (4)$$

where  $K_f^L$  is the longitudinal thermal conductivity of Gf,  $V' f$  is the volume fraction of Gf in the composite material, and  $t$  and  $D$  are the thickness and diameter of Gf, respectively.  $K_{foam}$  can be calculated with Eq. (3).

The calculated vs. the experimental results of longitudinal thermal conductivity for these composite foams are represented in **Figure 11a**. **Figure 11b** depicts the power dissipation densities of two Al/Gf composite foams (one with  $V' f = 0.54$  and another one with  $V' f = 0.34$ ) and a conventional aluminum foam (with a porosity volume fraction of 0.78) vs. airflow, obtained with the setup described in [8]. It is clear that proper designs of Al/Gf composite foams can reach power dissipation densities three times higher than those achieved with conventional aluminum foams.

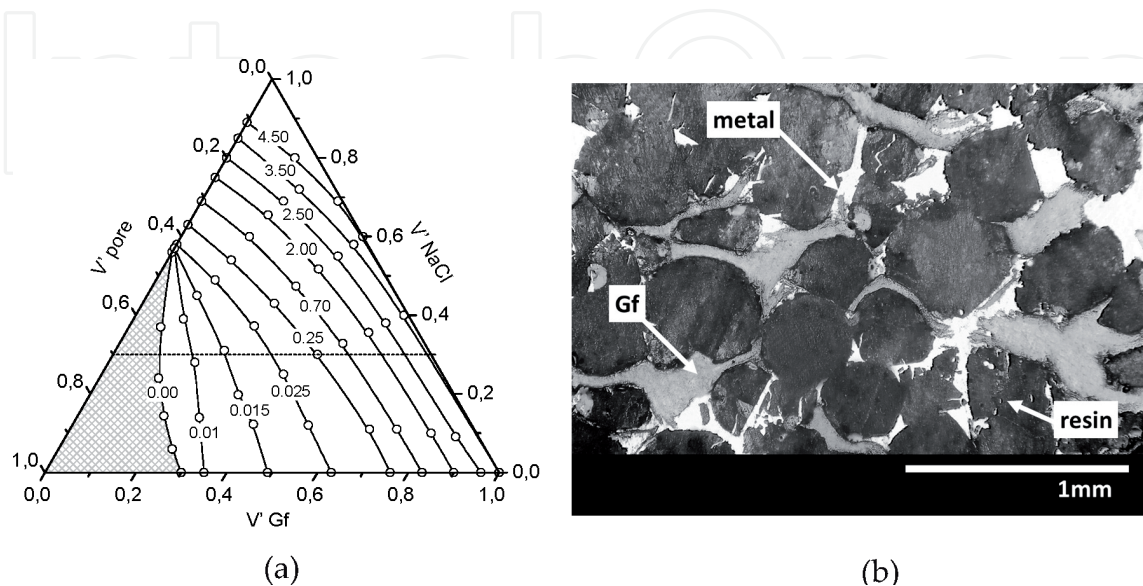


**Figure 10.**

(a) Preform composition ternary phase diagram as a function of compaction pressure (in MPa) and (b) photograph of an Al/Gf foam with homogeneous distribution of oriented Gf along the porous material. In (b) the pores were infiltrated with epoxy resin for a better polishing. Reproduced with permission from [13].

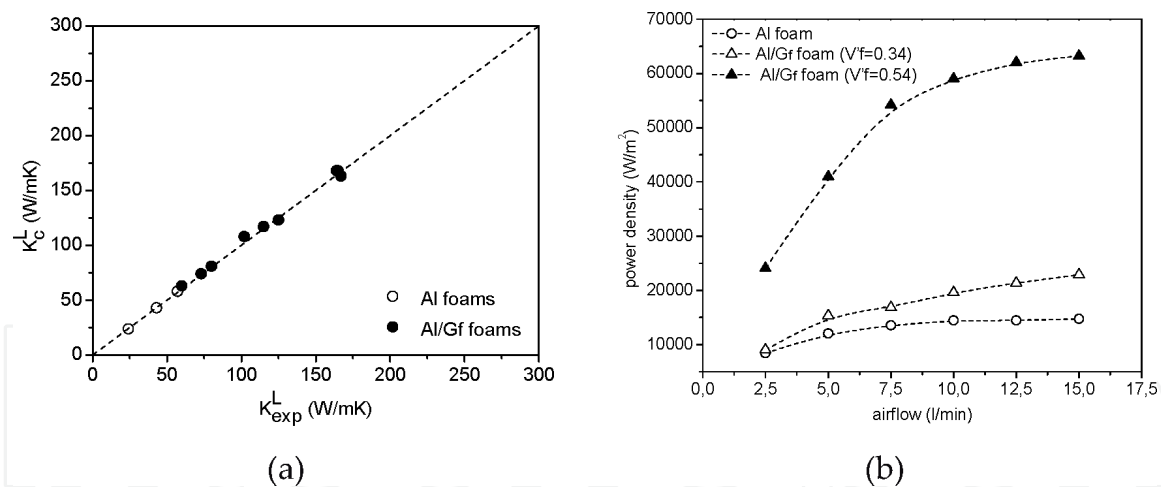


**Figure 11.** (a) Calculated vs. experimental thermal conductivities for different Al/Gf composite foams and (b) a comparison of power dissipation density as a function of airflow between some selected Al/Gf composite foams and a conventional aluminum foam. Graphit flakes dimensions: 1000  $\mu\text{m}$  average diameter and 20–45  $\mu\text{m}$  thickness. Partially reproduced from [13].

#### 4.1.3 Foams with guest phases

Open-pore foams containing guest phases in porous cavities is one of the latest developments in the design of foam materials that brings specific functionalities and opens niches for new applications [15, 16]. Depending on the nature of the guest phases or the combination of them, several applications can be considered for these materials such as adsorption of gases, adsorption of liquids or species in solution, catalysis, filters of inorganic or biological substances, and medical implantology. The processing route involves the generation of preforms by packaging particles coated with a sacrificial material (e.g., NaCl), their subsequent infiltration with a suitable precursor, and finally the dissolution of the sacrificial material. This results in open-pore foams in which the cavities contain other phases that provide certain functionalities. A distinctive feature is that there is no bond between the matrix and the guest phases, except for a simple contact generated by gravity, so that the interconnectivity of the pores remains assured. **Figure 12** shows SEM images of a guest particle coated with a sacrificial material (NaCl in this case) (a) and the same guest particle inside the pore cavity of a metal foam (b).

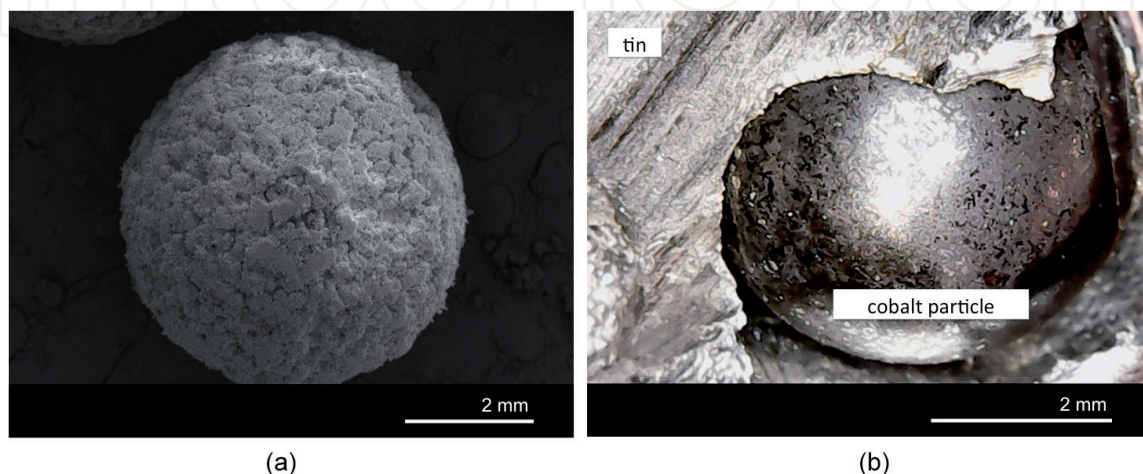


**Figure 12.** Cobalt sphere with NaCl coating (a) and cobalt sphere as guest phase inside a cavity of an open-pore tin foam (b). Reproduced from [15, 16].

These materials have not yet been widely characterized, but it is intuited that they have a great potential in the following applications:

- Thermal dissipation by forced convection: the presence of guest phases in the porous cavities alters the distribution of fluid flow lines inside the pores and generates a greater interaction of the fluid with the pore walls, which translates into increased fluid heating and consequently into greater heat dissipation power.
- Catalysis: the material allows catalytically active specimens to be housed in the guest phases and under certain conditions promotes non-laminar regimes in the passage of fluids through it, which notably increases its catalytic activity. In addition, this material can be considered multi-catalytic when different catalytic centers, supported on guest phases physically separated, are combined.
- Medical implantology: the material can act as an implant, allowing the in-growth of living tissue. The presence of guest phases with adsorbent capacity may be helpful to retain some substances with pharmacological activity that can be released in a controlled manner by desorption and thus avoid possible infections.

## 4.2 Composite foams with preload of new phases in the liquid precursor

### 4.2.1 Graphite/TiC nanocomposite foams

TiC-supported metals are interesting systems for catalytic applications. In [14] a new route was presented for the manufacturing of mesophase pitch foam materials containing TiC nanoparticles selectively distributed in two locations (**Figure 13**): in the foam struts (A zone) and at the pore surfaces (B zone). The particles of the struts act as catalysts of the graphitization process to which the mesophase pitch foams are subjected in order to considerably increase their thermal conductivity. The TiC particles on the surface allow transition metals with catalytic capacity to be supported.

As expected, it was found that the higher the TiC content in A zone, the greater the thermal conductivity of these open-pore multiphase foams (thermal

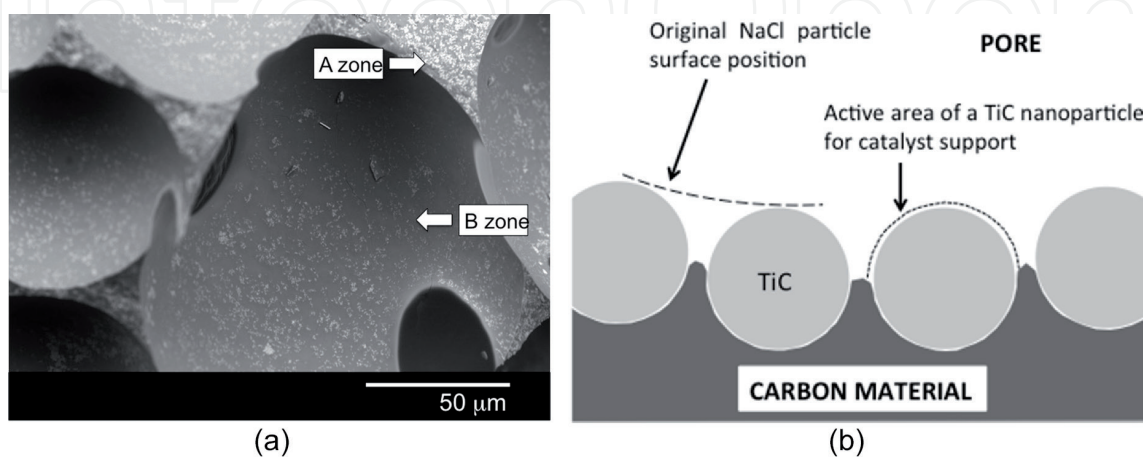


**Figure 13.**

(a) SEM image showing the location of TiC nanoparticles in the foam struts (A zone) and at the pore surfaces (B zone) and (b) a schematic drawing showing the TiC nanoparticles at the pore surface, which are not completely embedded in the carbon-based material. Reproduced with permission from [14].

conductivities up to 61 W/mK were measured for materials with 15% TiC in A zone and 45% pore surface coverage). The TiC particles at the pore surfaces do not modify the thermal conductivity of the foams, as they are not involved in the graphitization process. However, the higher the nanoparticle content at the pores, the greater the specific surface area of the foam, as the nanoparticles are only partially embedded in the mesophase pitch when infiltration takes place, as can be seen in **Figure 13b**.

#### *4.2.2 Metal/ceramic composite foams*

Composite foams are attractive because of their thermal properties, but also because they exhibit interesting mechanical properties when compared to their equivalent raw materials. Many research groups focused their efforts on modifying metal foam microstructures by adding particle reinforcements to enhance their mechanical properties. For that sake, Ni/SiC and Ni/Cu composite foams were proposed in literature [22]. They were manufactured by electrochemical (co)-deposition of the metal and the ceramic particles on polymeric templates. Stainless steel/titanium carbonitrides were also successfully prepared by the replication method [23].

AC3A aluminum alloy/SiC composite foams were manufactured by a similar synthesis route as that described in Section 3.2.2 [20]. The incorporation of the ceramic particles in the foam material strongly improved the compressive strength, energy absorption, and microhardness. The improvement of these properties was due to the modification of the microstructure and the increased strength at the locations where SiC particles were incorporated.

### **4.3 Finned foams**

Finned metal foams were also presented as new designs for thermal applications in [30, 31]. The multiphase open-pore materials developed by Bhattacharya and Mahajan [30] combine alternated parallel aluminum fins with 5 and 20 PPI aluminum foams joined with epoxy glue, as it was previously schematized in **Figure 4**. The results reported in [30] show that these finned foams enhance the heat transfer performance in comparison with conventional aluminum foams, being this increase proportional to the number of fins in the foam. Compared with equivalent aluminum foams, an increase of approximately 150% was reached when fine fins were incorporated. Despite the improved thermal performance of finned foams, the existent joints between components result in poor heat transfer among them. In order to improve the heat transfer between components, new finned foam structures with continuous matrix (no joints) were developed in the last years, and their main characteristics are detailed in next sections.

### **4.4 Monolithic finned foams**

To maximize heat transport between components, monolithic finned copper foams with different geometries of pores were fabricated by a new manufacturing process presented in [33]. 3D printed polymeric or wax patterns were used as sacrificial materials in an investment casting process. This process eliminates the need to restrict design geometries to shapes that can be easily separated from a reusable mold. Their structure, hence, allow these materials to be classified as a combination of monolithic materials with a continuous matrix (Section 3.2.4).

## 4.5 Composite finned foams

### 4.5.1 Aluminum/graphite flake composite finned foams

These multiphase materials were also inspired by those presented in [40, 41]. Preforms were prepared by uniaxial pressure packaging of alternating layers of graphite flakes and NaCl particles. Preforms were infiltrated by the gas pressure technique with liquid aluminum and later leached away by water dissolution.

In this type of preforms, there are no restrictions concerning percolation, as the structure could ideally be understood as composed of alternating porous NaCl and Gf monoliths. Even in the extreme case where the percentage of NaCl monoliths is negligible compared to that of Gf monoliths, the NaCl particles in the monolith still have enough coordination to be effectively removed by dissolution. Nevertheless, a compaction limit is detected for preforms prepared without external pressure as a result of the natural tendency of graphite flakes to lie on top of one another (**Figure 14a**). The resulting multiphase open-pore foams present microstructures with alternating layers of oriented graphite flakes and metal foam, as it is shown in **Figure 14b**.

For alternating layers of Al foam and Gf monoliths, the longitudinal thermal conductivity of the composite finned foams  $K_C^L$  can be estimated by the well-known Maxwell approach [13, 41]:

$$K_C^L = V' f \cdot K_f^L + (1 - V' f) \cdot K_{foam} \quad (5)$$

where the symbols have the same meaning as in Eq. (4) and  $K_{foam}$  is again calculated with Eq. (3).

Analytical values obtained from Eq. (5) are correlated with the experimental results in **Figure 15a**. As it can be seen, the model represented by Eq. (5) can reasonably predict the longitudinal thermal conductivities for the Al/Gf composite finned foams, which reach experimental values up to 290 W/mK. The power dissipation density results obtained under working conditions with the setup described in [8] are represented in **Figure 15b**. The experimental results show increments in power dissipation density up to 325% compared with conventional aluminum foams.

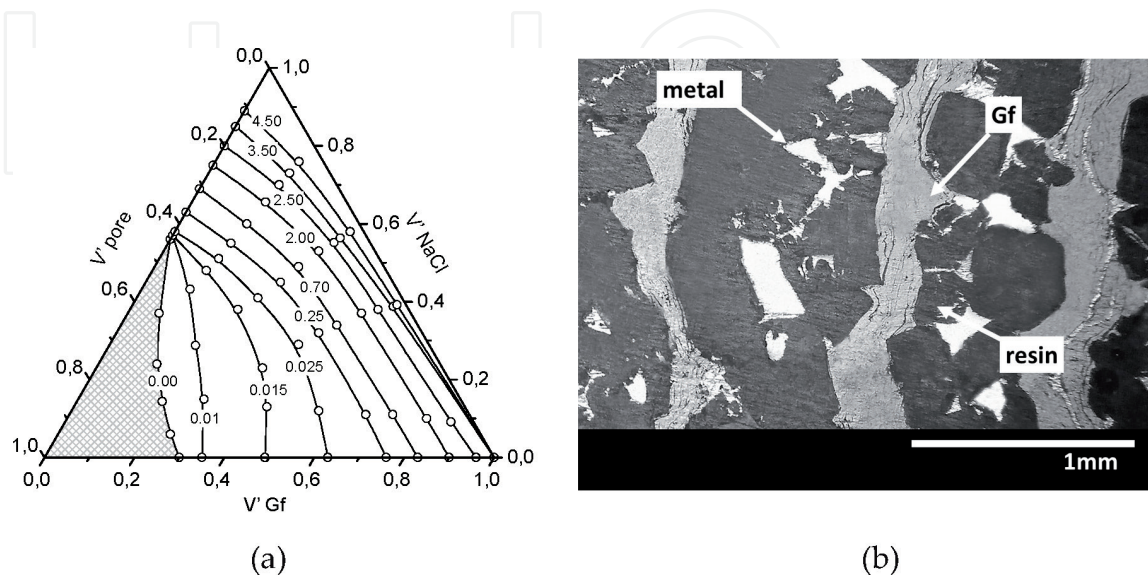


**Figure 14.** (a) Preform composition ternary phase diagram as a function of compaction pressure (in MPa) and (b) photograph of an Al/Gf foam with alternating layers of oriented graphite flakes and metal foam. Reproduced with permission from [13].

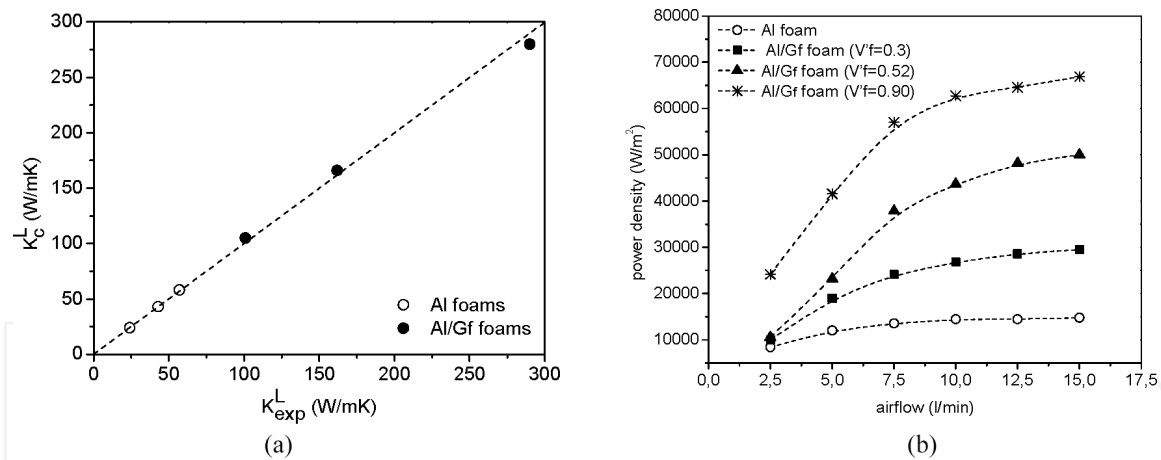


**Figure 15.**  
 (a) Calculated vs. experimental thermal conductivities for different Al foams and Al/Gf composite foams and (b) a comparison of power dissipation density as a function of airflow between some selected Al/Gf composite foams and a conventional aluminum foam. Graphite flake dimensions: 1000  $\mu\text{m}$  average diameter and 20–45  $\mu\text{m}$  thickness. Partially reproduced from [13].

## 5. Conclusions

This chapter reviews recent developments in the manufacture and characterization of multiphase foams developed by incorporation of new phases into open-pore foam materials. The new incorporated phases can significantly alter the macro-/microstructure of the starting materials or modify the pore surfaces to achieve new functionalities.

The incorporation of new phases into open-pore foams opens up a new range of properties in foam materials since improvements can be obtained in the mechanical, thermal, catalytic, or adsorptive properties, among others. The design and conception of multiphase open-pore foams seem to be a very suitable way to overcome the growing demands for very specific properties in some modern applications in sectors such as electronics, catalysis, or medical implantology.

## Acknowledgements

The authors acknowledge partial financial support from the Spanish Agencia Estatal de Investigación (AEI) and European Union (FEDER funds) through grant MAT2016-77742-C2-2-P.

## Conflict of interest

The authors declare no conflict of interest.

## Nomenclature

$D$	graphite flakes diameter (m)
Gf	graphite flakes
$h$	matrix/inclusion interface thermal conductance (W/m <sup>2</sup> K)
$K_C$	thermal conductivity of composite (W/mK)

$K_C^L$	longitudinal thermal conductivity of composite foam (W/mK)
$K_{exp}^L$	experimental thermal conductivity of composite foam (W/mK)
$K_f^L$	longitudinal thermal conductivity of graphite flakes (W/mK)
$K_{foam}$	thermal conductivity of foam (W/mK)
$K_m$	thermal conductivity of matrix (W/mK)
$K_r^{eff}$	effective thermal conductivity of inclusion (W/mK)
$K_r^{in}$	intrinsic thermal conductivity of inclusion (W/mK)
$p$	polarization factor of inclusion
$r$	radius of inclusion (m)
$t$	graphite flake thickness (m)
$V$	volume fraction of inclusions
$V_f$	volume fraction of graphite flakes
$V_p$	volume fraction of pores
$X_i$	fraction of i inclusion type in the total amount of inclusions

## Author details

Lucila Paola Maiorano Lauría<sup>1</sup> and José Miguel Molina Jordá<sup>2\*</sup>

<sup>1</sup> University Materials Institute of Alicante (IUMA), University of Alicante, Alicante, Spain

<sup>2</sup> Inorganic Chemistry Department, University Materials Institute of Alicante (IUMA), University of Alicante, Alicante, Spain

\*Address all correspondence to: [jmmj@ua.es](mailto:jmmj@ua.es)

## IntechOpen

© 2019 The Author(s). Licensee IntechOpen. This chapter is distributed under the terms of the Creative Commons Attribution License (<http://creativecommons.org/licenses/by/3.0>), which permits unrestricted use, distribution, and reproduction in any medium, provided the original work is properly cited. 

## References

- [1] Banhart J. Manufacture, characterisation and application of cellular metals and metal foams. *Progress in Materials Science*. 2001;**46**:559-632
- [2] Hammel EC, Ighodaro OLR, Okoli OI. Processing and properties of advanced porous ceramics: An application based review. *Ceramics International*. 2014;**40**:15351-15370
- [3] Khemani KC. *Polymeric Foams: An Overview*. Washintong, DC: ASC Symposium Series, American Chemical Society; 2009. pp. 1-7
- [4] Singh S, Bhatnagar N. A survey of fabrication and application of metallic foams (1925-2017). *Journal of Porous Materials*. 2018;**25**:537-554
- [5] Lewis G. Properties of open-cell porous metals and alloys for orthopaedic applications. *Journal of Materials Science. Materials in Medicine*. 2013;**24**:2293-2325
- [6] Schelling PK, Shi L, Goodson KE. Managing heat for electronics. *Materials Today*. 2005;**8**:30-35. DOI: 10.1016/s1369-7021(05)70935-4
- [7] Mallik S, Ekere N, Best C, Bhatti R. Investigation of thermal management materials for automotive electronic control units. *Applied Thermal Engineering*. 2011;**31**:355-362. DOI: 10.1016/j.applthermaleng.2010.09.023
- [8] Molina-Jordá JM. Multi-scale design of novel materials for emerging challenges in active thermal management: Open-pore magnesium-diamond composite foams with nano-engineered interfaces. *Composites Part A: Applied Science and Manufacturing*. 2018;**105**:265-273. DOI: 10.1016/j.compositesa.2017.11.020
- [9] Shih WH, Chiu WC, Hsieh WH. Height effect on heat-transfer characteristics of aluminum-foam heat sinks. *Journal of Heat Transfer*. 2006;**128**:530
- [10] Zaragoza G, Goodall R. Development of a device for the measurement of thermal and fluid flow properties of heat exchanger materials. *Measurement: Journal of the International Measurement Confederation*. 2014;**56**:37-49
- [11] Zaragoza G, Goodall R. Metal foams with graded pore size for heat transfer applications. *Advanced Engineering Materials*. 2013;**15**: 123-128
- [12] Mancin S, Zilio C, Diani A, Rossetto L. Air forced convection through metal foams: Experimental results and modeling. *International Journal of Heat and Mass Transfer*. 2013;**62**:112-123. DOI: 10.1016/j.ijheatmasstransfer.2013.02.050
- [13] Maiorano LP, Molina JM. Challenging thermal management by incorporation of graphite into aluminium foams. *Materials and Design*. 2018;**158**:160-171. DOI: 10.1016/j.matdes.2018.08.026
- [14] Molina-Jordá JM. Mesophase pitch-derived graphite foams with selective distribution of TiC nanoparticles for catalytic applications. *Carbon*. 2016;**103**:5-8. DOI: 10.1016/j.carbon.2016.02.051
- [15] Molina Jorda JM. Spanish Patent P201730890. 2017
- [16] Molina-Jorda JM. PCT Patent PCT/ES2018/070474. 2018
- [17] Körner C, Singer RF. Processing of metal foams—Challenges and opportunities. *Advanced Engineering Materials*. 2000;**2**:159-165. DOI: 10.1002/

(SICI)1527-2648(200004)2:4<159::AID-ADEM159>3.0.CO;2-O

[18] Prieto R, Louis E, Molina JM. Fabrication of mesophase pitch-derived open-pore carbon foams by replication processing. *Carbon*. 2012;**50**:1904-1912. DOI: 10.1016/j.carbon.2011.12.041

[19] Alizadeh M, Mirzaei-Aliabadi M. Compressive properties and energy absorption behavior of Al-Al<sub>2</sub>O<sub>3</sub> composite foam synthesized by space-holder technique. *Materials and Design*. 2012;**35**:419-424. DOI: 10.1016/j.matdes.2011.09.059

[20] Wichianrat E, Boonyongmaneerat Y, Asavavisithchai S. Microstructural examination and mechanical properties of replicated aluminium composite foams. *Transactions of Nonferrous Metals Society of China (English Edition)*. 2012;**22**:1674-1679

[21] Bouwhuis BA, McCrea JL, Palumbo G, Hibbard GD. Mechanical properties of hybrid nanocrystalline metal foams. *Acta Materialia*. 2009;**57**:4046-4053

[22] Mikutski V, Smorygo O, Shchurevich D, Marukovich A, Ilyushchenko A, Gokhale A. Open-cell metal-SiC composite foams made by electrolytic code position on polyurethane substrates. *Powder Metallurgy and Metal Ceramics*. 2014;**52**:545-550

[23] Bakan HI, Korkmaz K. Synthesis and properties of metal matrix composite foams based on austenitic stainless steels—Titanium carbonitrides. *Materials and Design*. 2015;**83**:154-158. DOI: 10.1016/j.matdes.2015.06.016

[24] Antenucci A, Guarino S, Tagliaferri V, Ucciardello N. Improvement of the mechanical and thermal characteristics of open cell aluminum foams by the electrodeposition of Cu. *Materials and Design*. 2014;**59**:124-129

[25] Devivier C, Tagliaferri V, Trovalusci F, Ucciardello N. Mechanical characterization of open cell aluminium foams reinforced by nickel electro-deposition. *Materials and Design*. 2015;**86**:272-278. DOI: 10.1016/j.matdes.2015.07.078

[26] Edouard D, Ivanova S, Lacroix M, Vanhaecke E, Pham C, Pham-Huu C. Pressure drop measurements and hydrodynamic model description of SiC foam composites decorated with SiC nanofiber. *Catalysis Today*. 2009;**141**:403-408

[27] Wang W, Burgueño R, Hong JW, Lee I. Nano-deposition on 3-D open-cell aluminum foam materials for improved energy absorption capacity. *Materials Science and Engineering A*. 2013;**572**:75-82. DOI: 10.1016/j.msea.2013.02.032

[28] Sun Y, Burgueño R, Vanderklok AJ, Tekalur SA, Wang W, Lee I. Compressive behavior of aluminum/copper hybrid foams under high strain rate loading. *Materials Science and Engineering A*. 2014;**592**:111-120

[29] Luo Y, Yu S, Liu J, Zhu X, Luo Y. Compressive property and energy absorption characteristic of open-cell SiCp/AlSi9Mg composite foams. *Journal of Alloys and Compounds*. 2010;**499**:227-230. DOI: 10.1016/j.jallcom.2010.03.172

[30] Bhattacharya A, Mahajan RL. Finned metal foam heat sinks for electronics cooling in forced convection. *Journal of Electronic Packaging*. 2002;**124**:155

[31] Feng SS, Kuang JJ, Wen T, Lu TJ, Ichimiya K. An experimental and numerical study of finned metal foam heat sinks under impinging air jet cooling. *International Journal of Heat and Mass Transfer*. 2014;**77**:1063-1074. DOI: 10.1016/j.ijheatmasstransfer.2014.05.053

- [32] Wang J, Kong H, Xu Y, Wu J. Experimental investigation of heat transfer and flow characteristics in finned copper foam heat sinks subjected to jet impingement cooling. *Applied Energy*. 2019;**241**:433-443. DOI: 10.1016/j.apenergy.2019.03.040
- [33] Krishnan S, Herson D, Hodes M, Mullins J, Lyons AM. Design of complex structured monolithic heat sinks for enhanced air cooling. *IEEE Transactions on Components, Packaging and Manufacturing Technology*. 2012;**2**:266-277
- [34] Molina-Jordá JM. Design of composites for thermal management: Aluminum reinforced with diamond-containing bimodal particle mixtures. *Composites Part A: Applied Science and Manufacturing*. 2015;**70**:45-51. DOI: 10.1016/j.compositesa.2014.12.006
- [35] Molina-Jordá JM. Nano- and micro-/meso-scale engineered magnesium/diamond composites: Novel materials for emerging challenges in thermal management. *Acta Materialia*. 2015;**96**:101-110. DOI: 10.1016/j.actamat.2015.06.003
- [36] Molina JM, Saravanan RA, Arpón R, García-Cordovilla C, Louis E, Narciso J. Pressure infiltration of liquid aluminium into packed SiC particulate with a bimodal size distribution. *Acta Materialia*. 2002;**50**:247-257
- [37] Molina-Jordá JM. SiC as base of composite materials for thermal management. In: Mukherjee M, editor. *Silicon Carbide— Materials, Processing and Applications in Electronic Devices*. Rijeka: IntechOpen; 2011. pp. 115-140. DOI: 10.5772/57353
- [38] Molina JM, Narciso J, Weber L, Mortensen A, Louis E. Thermal conductivity of Al-SiC composites with monomodal and bimodal particle size distribution. *Materials Science and Engineering A*. 2008;**480**:483-488. DOI: 10.1016/j.msea.2007.07.026
- [39] Hsieh WH, Wu JY, Shih WH, Chiu WC. Experimental investigation of heat-transfer characteristics of aluminum-foam heat sinks. *International Journal of Heat and Mass Transfer*. 2004;**47**:5149-5157. DOI: 10.1016/j.ijheatmasstransfer.2004.04.037
- [40] Prieto R, Molina JM, Narciso J, Louis E. Fabrication and properties of graphite flakes/metal composites for thermal management applications. *Scripta Materialia*. 2008;**59**:11-14. DOI: 10.1016/j.scriptamat.2008.02.026
- [41] Prieto R, Molina JM, Narciso J, Louis E. Thermal conductivity of graphite flakes-SiC particles/metal composites. *Composites Part A: Applied Science and Manufacturing*. 2011;**42**:1970-1977. DOI: 10.1016/j.compositesa.2011.08.022